Proceedings 10th NUMGE 2023
10th European Conference on Numerical Methods in Geotechnical Engineering
Zdravkovic L, Kontoe S, Taborda DMG, Tsiampousi A (eds)

https://doi.org/10.53243/NUMGE2023-144

Modelling rockfall by a novel FEM-DEM coupling approach with explicitly considering geomaterial heterogeneity

B. Gong[1] , T. Zhao[1]

[1]*Department of Civil and Environmental Engineering, Brunel University London, London, UK*

ABSTRACT: The finite element method (FEM), the implicit discrete element method (DEM) and the statistical strength theory were coupled to model the meso-macro cross-scale failure mechanism of rock masses and reveal the impact characteristics of rockfalls influenced by rock heterogeneity. In the proposed method, the automatic transformation of rock materials from continuous medium to discontinuous medium can be realized. Meanwhile, the spatial inhomogeneity of rock properties can be considered by the specific distribution function. After verifying the effectiveness, the coupled method was applied to investigate rock failure and rockfall. The results show that it is the continuous process of stress build-up, stress shadow and stress transfer that leads to the gradual development of cracks and the macro failure of the rocks containing fissures and holes; the horizontal movement distance of the largest falling rock fluctuates when the nonuniform coefficient increases from 1.01 to 4, indicating that the strong material heterogeneity will lead to the high uncertainty of fragment distribution; this distance decreases greatly when the nonuniform coefficient researched 5 and 6 because one obvious major falling block can form, and the trajectory of the large block is relatively regular.

Keywords: landslide; progressive failure; FEM-DEM coupling; heterogeneity; numerical modelling

1 INTRODUCTION

Rockfall is a significant geologic hazard that poses a serious threat to both life and property. Geotechnical engineering is tasked with ensuring the safety and stability of slopes. To mitigate the risk of rockfalls, qualitative and quantitative assessments of slope stability are necessary. In fact, it is essential to prevent accidents resulting from rock failure wherever possible. Unfortunately, fatal rockfalls still occur.

Describing the formation, propagation, and penetration of fractures is a challenging topic due to the complexity of rock media. Rocks at the micro level are aggregates of mineral grains that are embedded together through crystallization. At the meso level, rocks are aggregates of mineral particles bonded together through cement. Due to the effect of tectonic movement of the Earth's upper crust, the coupling action of internal liquid and gaseous substances, and long-term weathering and erosion, rock media typically contains many holes, dikes, micro-cracks, joints, etc. across micro, meso, and macro levels. This complexity makes it challenging to represent them using traditional mathematical approaches.

In this study, the finite element method (FEM), implicit discrete element method (DEM) and the statistical strength theory were coupled to model the meso- macro cross-scale failure mechanism of rock masses and reveal the impact characteristics of rockfalls influenced by material heterogeneity.

2 METHODOLOGY

2.1 Characterization of material heterogeneity

The heterogeneity of material properties is one of the critical features of rocks that greatly impacts their deformation modes and failure characteristics (Manthei 2005). To model rock mass, the proposed approach employs a number of representative volume elements (RVEs) at the mesoscopic level. The parameter values of the RVEs are assumed to follow a specific statistical distribution function according to the statistical strength theory to describe the effect of mesoscopic rock heterogeneity on complicated macroscopic responses. Researchers have widely used the Weibull distribution to capture the distribution rules of rock mechanical parameters (Weibull 1951; Basu *et al*. 2009; Sanchidrian *et al*. 2014; Fu *et al*. 2017; Nassar *et al*. 2018), and it is therefore used in the proposed method. The Weibull distribution can be expressed as follows:

$$f(u) = \frac{m}{u_0}(\frac{u}{u_0})^{m-1} exp\ -(\frac{u}{u_0})^m \quad (1)$$

where u represents the specific mechanical parameter of RVEs, *e.g.* strength, elastic modulus, friction angle; u_0 represents the mean value of the parameter p; m represents the nonuniform coefficient. For various nonuniform coefficients m, the probability density curves of the mechanical parameter u are shown in Figure 1.

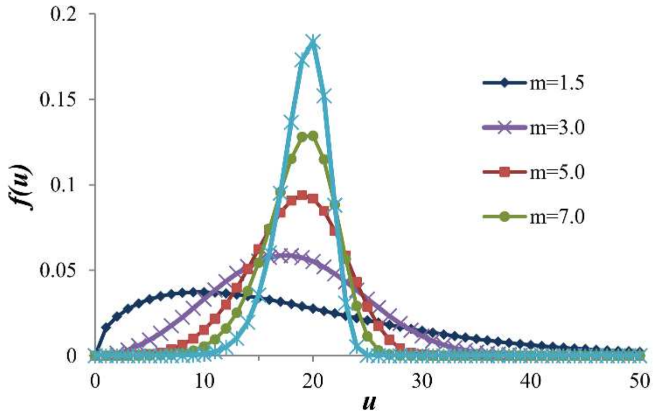

Figure 1. Weibull probability densities under various nonuniform coefficients m

2.2 The constitutive relation

According to the statistical-damage theory, the parameter values of these RVEs follow the specific statistical distribution function. Simultaneously, at the initial stage, the constitutive relationship of a RVE keeps linear elastic. When the threshold stress is reached, the strength criterion will be met, and the behaviour of damaged elements will be strain-softening. When a RVE is subjected to uniaxial load, such as uniaxial compression or uniaxial tension, the related stress-strain correlation could be described by the curve as shown in Figure 2. While the constitutive relationship of RVEs is relatively simple, the nonuniform distribution of parameters can result in a very complex macroscopic mechanical response of the model.

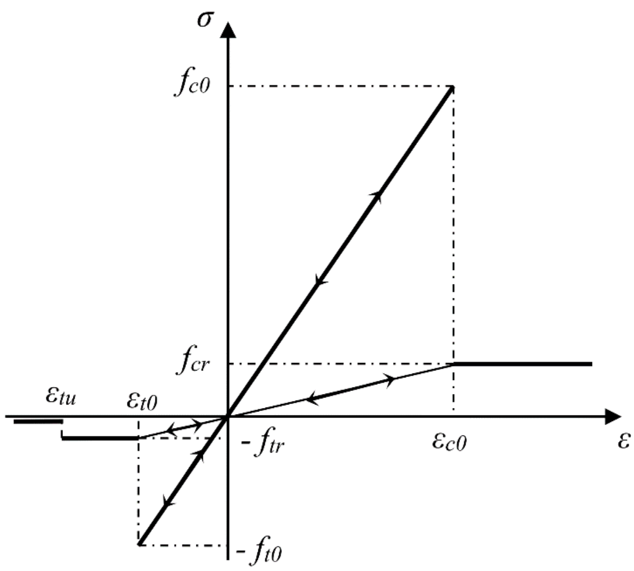

Figure 2. Constitutive relation of a RVE sufering uni-axial compression and tension

The elastic modulus of a damaged element may continuously degenerate according to the damage intensity, as follows:

$$E = (1 - \omega)E_0 \tag{2}$$

where ω represents the damage factor; E and E_0 represent the element elastic moduli at damaged and initial undamaged states, respectively. Note that in this study, the RVEs and the corresponding damage are assumed to be isotropic, which means that E, E_0 and ω are scalars (Tang *et al*. 2002).

If a RVE is suffering the compression-shear stress state, the Mohr-Coulomb strength criterion could be triggered as follows:

$$f_{c0} \le \sigma_1 - \frac{1+\sin\varphi}{1-\sin\varphi}\sigma_3 \tag{3}$$

where f_{c0} represents the uniaxial compressive strength; φ represents the internal friction angle; σ_1 and σ_3 represent the maximum and minimum principal stresses, respectively.

If a RVE is suffering the tensile load, the maximum tensile strain criterion could be satisfied as follows:

$$\sigma_3 \le f_{t0} \tag{4}$$

where f_{t0} represents the uniaxial tensile strength.

3 RESULTS

3.1 Uniaxial compression

In order to verify the performance of the proposed method in simulating the initiation, propagation and nucleation of rock cracks, a rock sample of 150 mm height and a diameter of 75 mm was compressed under uniaxial compression loading. The heterogeneity of material properties has been taken into account in model generation.

Table 1 Physical-mechanical properties of the rock specimen

Parameter	Value
Density ρ (kg/m^3)	2700
Elastic modulus E (GPa)	50
Poisson's ratio v	0.2
Nonuniform coefficient m	1.5
Cohesion c (MPa)	100
Internal friction angle φ (°)	20
Uniaxial tensile strength f_{t0} (MPa)	7

The physical and mechanical parameters are listed in Table 1, and the elastic modulus, cohesion and tensile strength were assumed to follow a Weibull distribution. The model was divided into 8,100 elements, with the bottom boundary fixed along the normal direction, and the downward loading displacement-control of 0.02 mm/s. This loading rate can be considered as quasi-static/static, and the dynamic effect can be ignored (Ha *et al*. 2015; Li and Wong 2012).

Figure 3 shows the crack initiation and propagation processes at different compressive stages. Figure 3 (a) shows that at the beginning of loading, due to nonuniform distribution of material properties, the finite elements at some weak regions were damaged firstly. These damaged elements not only represented the potential position of crack initiation, but also affected the subsequent crack propagation process. There are two separate cracks occurring in the sample. The longer one is located at the lower right side; the other is shorter at the middle right side. Additionally, there is an obvious stress concentration at the ends of the two main cracks, and it is the concentrated high stress that promoted the continuous upward and downward development of the cracks. With the evolution of cracks, the concentrated stresses were released and transferred to the new crack tips. This process of stress build-up, stress shadow and stress transfer leads to the gradual growth of cracks.

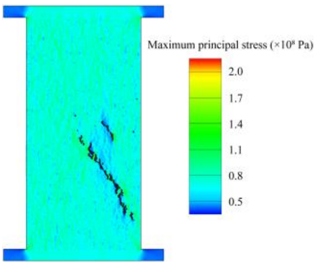

(a) ε_a = 1.96×10^{-3}

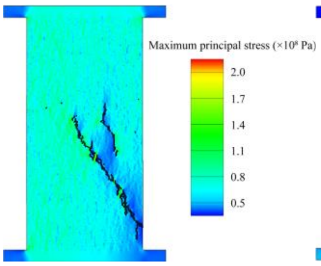

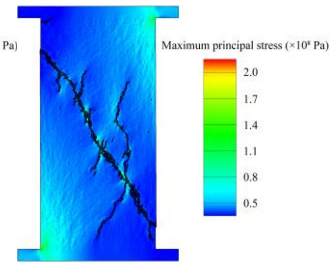

(b) ε_a = 1.97×10^{-3} *(c) ε_a = 2.21×10^{-3}*

Figure 3. Rock failure process with the axial strain (ε_a) increasing under uniaxial compression

Furthermore, with the load increasing, the two independent cracks keep growing, and the longer crack reaches the right boundary of the sample, as shown in Figure 3 (b). Moreover, due to the influence of material nonuniformity, the strength of local rock may be larger than its surrounding rocks. This mechanism results in the formation of the small isolated block near the boundary at the lower right corner. Simultaneously, the high stresses occurred in that region. This phenomenon represents an important advantage of the developed program with the coupled solving algorithm, *i.e.*, the deformable rock could be broken into fragments without the assumptions on where and how the cracks are initiated and propagated. Figure 3 (c) shows that after the two main cracks nucleated, the newly formed crack continued to develop towards the upper left corner, and finally separated the original rectangular specimen into two large pieces. Additionally, the mechanical sliding between two blocks along the interface is allowed in the developed program, and the simulated failure mode agrees well with the other studies (Wang *et al.* 2017; Tang *et al.* 2000).

3.2 Fracture of rock containing fissure and hole

In nature, rock mass usually contains many discontinuities, such as joints, fissures and holes, which often govern the mechanical properties and failure behaviours. Considering such defects are the potential sources of crack creation and will affect the propagation path and coalescence mode of cracks, they are generally regarded as the dominant factors of rock failure. Thus, it is essential to investigate the characteristics of crack evolution and mechanical mechanisms of rock mass containing flaws for preventing geological disasters. Two kinds of flaws primarily exist, *i.e.*, crack-like flaws and hole-like flaws (Zhou *et al*. 2017). Additionally, for rock mass containing hole-like flaws, most studies focused on the fracturing behaviour under uniaxial compression, whereas knowledge about shearing-induced fractures is relatively limited (Han *et al*. 2020). However, the shear failure also commonly appears in rock slopes.

In this section, three kinds of fissure-hole models including fissure-square hole, fissure-elliptical hole, and fissure-circular hole were considered. The material elastic modulus, Poisson's ratio, cohesion, internal friction angle, uniaxial tensile strength and nonuniform coefficient were 30 GPa, 0.3, 30 MPa, 30°, 10 MPa, 5, respectively. The models with the size of 0.1 m × 0.2 m were divided into around 80,000 elements.The top of the model was applied with a stress of 1 MPa, and the bottom was fixed along the normal direction. The upper half of the left side and the lower half of the right side were loaded with a ratio of 0.005 mm/s. The simulated results are as shown in Figure 4.

From Figures 4 (a) and (b), we can see that at the beginning of load, four cracks generate at the left and right corners of the squares and the tips of the side fissures due to the high tensile stress concentrations. However, it is worth noting that the compressive stress concentrated areas exist near the tips of the four fissures of the squares. Because the compression resistance of the rock is greater than its tension resistance, no crack occurs at these tips. While the load increases, the rocks between the two squares are seriously damaged, leading to the rock bridge coalescence. In addition, there are two large blocks forming between the side fissures and the squares.

From Figures 4 (c) and (d), it can be seen that at the beginning of shearing, four cracks are created at the left and right corners of the ellipses and the tips of the side fissures where the concentrated tensile stresses are relatively high. Simultaneously, it is clear that there are high tensile stresses existing at the tips of the new cracks.

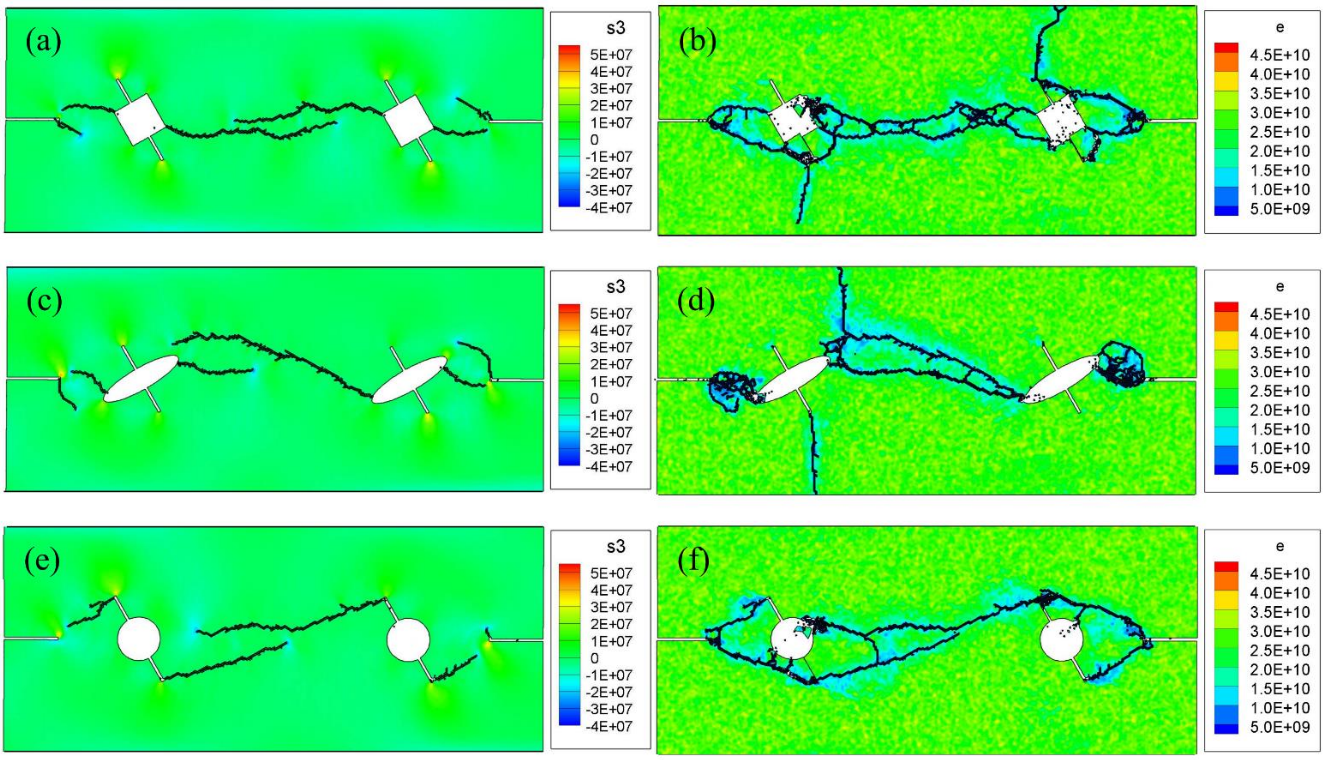

Figure 4. Shear failure process and mode of rock containing fissure-hole with different shapes: (a), (c), (e) are minor principal stress contours (Unit: Pa); (b), (d), (f) are elastic modulus contours (Unit: Pa)

Actually, when the concentrated tensile stresses satisfied the strength criterion, the new cracks initiated. At the same time, the formation of cracks resulted in the release of the concentrated stresses. Then, the released stresses transferred to the tips of the new cracks and built up again. It is the process of stress build-up, stress shadow and stress transfer that leads to the continuous development of cracks. Later, the rock bridge coalesces between the ellipses, and the rocks between the side fissures and the ellipses damage seriously.

From Figures 4 (e) and (f), we can see that at the beginning of shear load, four cracks initiate at the tips of the fissures crossing the circles, which is different from the fissure-square and fissure-elliptical hole models due to the various stress distributions. Furthermore, the cracks at the tips of the side fissures appear later that the four cracks. With the shear increasing, the cracks at the middle gradually propagate and coalesce, and the rock bridges between the fissures and circles are finally broken, promoting the macro failure of the model.

3.3 Rockfall impact

Rockfall appears frequently along highways especially in mountainous areas, which may cause unpredictable loss of life and property. The related failure analysis is important for the disaster prevention and mitigation. To investigate the rock rockfall impact, the corresponding models were established. The height of the slope was 140 m, and the width of the road was 15 m. Note that in this case, a falling rock is pre-set at the top of the slope.

The elastic modulus, Poisson's ratio, density, cohesion, internal friction angle and uniaxial tensile strength of the unstable rock formation were 25.5 GPa, 0.25, 2600 kg/m^3, 55 MPa, 27°, 40 MPa, respectively. Besides, as mentioned above, the heterogeneity plays a critical role in governing the nonlinear deformation and failure pattern of rocks. To study the influence of material heterogeneity on rockfall, six nonuniform coefficients were considered, *i.e.*, the nonuniform coefficient m (>1) equalled 1.01, 2, 3, 4, 5 and 6, respectively. The model consists of around 30,000 elements. The left side, right side and bottom were fixed along the corresponding normal direction, and the top was free. The simulated results are shown in Figure 5.

From Figure 5, it can be seen that the falling rock was broken into many small pieces after hitting the upper platform, but the degree of fragmentation is different with the nonuniform coefficient increasing. A higher nonuniform coefficient means a more uniform rock media. Furthermore, as we know, the strength of the elements are more likely to concentrate near the mean strength, indicating that the macro strength will increase with the growth of nonuniform coefficient. This explains the reason why the degree of fragmentation is influenced by the nonuniform coefficient. Then, the road is attacked by the falling rocks. On the one hand, the impact may cause direct damage to people and vehicles using the road. On the other hand, the rock debris may block the traffic. The impact effect could cause the strong stress redistribution, and the high impact stress might destroy the road.

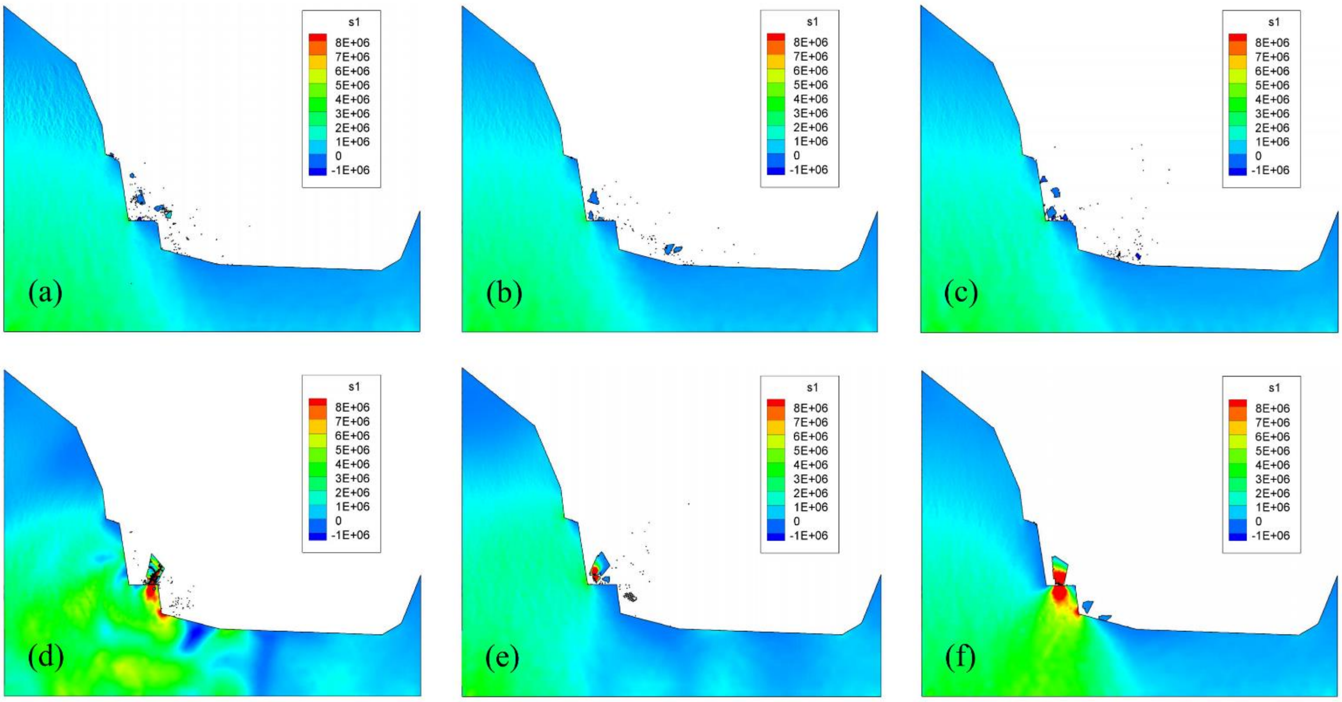

Figure 5. Rockfall with different nonuniform coefficients by major principal stress contour (Unit: Pa): (a) m = 1.01; (b) m = 2; (c) m = 3; (d) m = 4; (d) m = 5; (f) m = 6

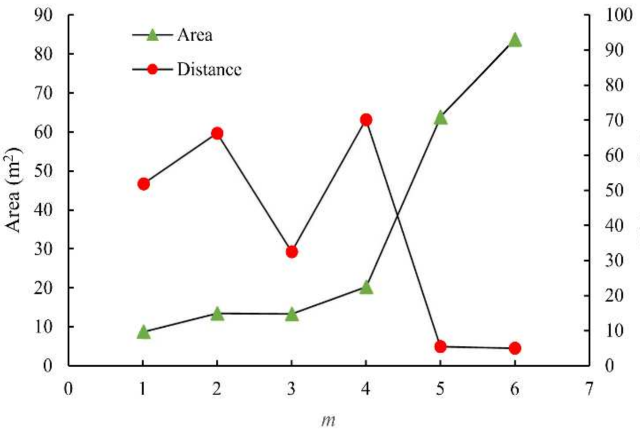

Figure 6. Area and distance of the largest rock under different nonuniform coefficients m

Figure 6 displays the area and horizontal distance to Point A of the largest rock after the whole rockfall impact, from which it can be seen that the area of the largest rock rises up gradually with the nonuniform coefficient increasing. Namely, the growth of nonuniform coefficient leads to the macro strength increase of the initial falling rock, therefore resulting in the area increase of the largest rock. Meanwhile, the horizontal movement distance of the largest rock fluctuates when the nonuniform coefficient increases from 1.01 to 4. However, this distance decreases greatly when the nonuniform coefficient researched 5 and 6. This phenomenon is because when the nonuniform coefficient is between 1.01 and 4, the degree of fragmentation is relatively large, and the areas of the rock fragments are relatively even and small, increasing the uncertainty of block distribution. Namely, the strong material heterogeneity will lead to the high uncertainty of fragment distribution. When the nonuniform coefficient grows up to 5 and 6, one obvious major block can form, and the trajectory of the large block is relatively regular.

4 CONCLUSIONS

The following conclusions can be drawn:

(1) The developed numerical method can be used for multiscale modelling of progressive slope failure. Furthermore, the occurrence of cracks can be caused by high concentrated stresses, and the formation of cracks would result in the release of the concentrated stresses. Then, the released stresses could transfer to the tips of the newly formed cracks and built up again. It is the gradual process of stress build-up, stress shadow and stress transfer that leads to the continuous development of cracks and the macro failure of the rocks containing fissures and holes.

(2) For rockfall, the area of the largest rock rises up gradually with the nonuniform coefficient *m* increasing. However, the horizontal movement distance of the largest rock fluctuates when *m* increases from 1.01 to 4. Namely, the strong material heterogeneity will lead to the high uncertainty of fragment distribution.

Furthermore, this distance decreases greatly when the nonuniform coefficient researches 5 and 6 because one obvious major block can form, and the trajectory of the large block is relatively regular.

5 ACKNOWLEDGEMENTS

This work was supported by the UK Engineering and Physical Sciences Research Council (EPSRC) New Investigator Award (No. EP/V028723/1). The datasets generated and analysed here are available upon request.

6 REFERENCES

Basu, B., Tiwari, D., Kundu, D., Prasad, R. 2009. Is Weibull distribution the most appropriate statistical strength distribution for brittle materials? *Ceramics International* **35(1)**, 237–246.

Fu, J.W., Zhang, X.Z., Zhu, W.S., Chen, K., Guan, J.F. 2017. Simulating progressive failure in brittle jointed rock masses using a modified elastic-brittle model and the application. *Engineering Fracture Mechanics* **178**, 212–230.

Han, W., Jiang, Y.J., Luan, H.J., Du, Y.T., Zhu, Y.G., Liu, J.K. 2020. Numerical investigation on the shear behavior of rock-like materials containing fissure-holes with FEM-CZM method. *Computers and Geotechnics* **125**, 103670.

Ha, Y.D., Lee, J., Hong, J.W. 2015. Fracturing patterns of rock-like materials in compression captured with peridynamics. *Engineering Fracture Mechanics* **144**, 176–193.

Sanchidrian, J.A., Ouchterlony, F., Segarra, P., Moser, P. 2014. Size distribution functions for rock fragments. *International Journal of Rock Mechanics & Mining Sciences* **71**, 381–394.

Shimizu, H., Koyama, T., Ishida, T., Chijimatsu, M., Fujita, T., Nakama, S. 2010. Distinct element analysis for Class II behavior of rocks under uniaxial compression. *International Journal of Rock Mechanics & Mining Sciences* **47(2)**, 323–333.

Tang, C.A., Tham, L.G., Lee, P.K.K., Yang, T.H., Li, L.C. 2002. Coupled analysis of flow, stress and damage (FSD) in rock failure. *International Journal of Rock Mechanics & Mining Sciences* **39(4)**, 477–489.

Tang, C.A., Than, L.G., Lee, P.K.K, Tsui, Y., Liu, H. 2000. Numerical studies of the influence of microstructure on rock failure in uniaxial compression–Part II: constraint, slenderness and size effect. *International Journal of Rock Mechanics and Mining Sciences* **37**, 571–583.

Li, H., Wong, L.N.Y. 2012. Influence of flaw inclination angle and loading condition on crack initiation and propagation. *International Journal of Solids and Structures* **49(18)**, 2482–2499.

Manthei, G. 2005. Characterization of acoustic emission sources in a rock salt specimen under triaxial compression. *Bulletin of the Seismological Society of America* **95(5)**, 1674–1700.

Nassar, M., Afify, A.Z., Dey, S., Kumar, D. 2018. A new extension of Weibull distribution: Properties and different methods of estimation. *Journal of Computational and Applied Mathematics* **336**, 439–457.

Wang, Y., Zhou, X., Shou, Y. 2017. The modeling of crack propagation and coalescence in rocks under uniaxial compression using the novel conjugated bond-based peridynamics. *International Journal of Mechanical Sciences* **128-129**, 614–643.

Weibull, W. 1951. A statistical distribution function of wide applicability. *Journal of applied mechanics* **103(730)**, 293–297.

Zhou, Z., Tan, L., Cao, W., Zhou, Z., Cai, X. 2017. Fracture evolution and failure behaviour of marble specimens containing rectangular cavities under uniaxial loading. *Engineering Fracture Mechanics* **184**, 183–201.